Design of pressure-sensitive adhesive suitable for the preparation of transdermal patches by hot-melt printing

Umberto M. Musazzi[1], Marco A. Ortenzi[2,3], Chiara G.M. Gennari[1], Antonella Casiraghi[1], Paola Minghetti[1], Francesco Cilurzo[1*]

[1] Department of Pharmaceutical Sciences, Università degli Studi di Milano - via G. Colombo 71 – 20133 Milan (Italy)

[2]Department of Chemistry, Università degli Studi di Milano, Via Golgi 19-20133 Milan, Italy

[3]CRC Materiali Polimerici (LaMPo), Department of Chemistry, Università degli Studi di Milano, Via Golgi 19-20133 Milan, Italy

*** to whom the correspondence should be sent:**

Prof. Francesco Cilurzo, PhD

Department of Pharmaceutical Science

Università degli Studi di Milano

Via Giuseppe Colombo, 71

20133 Milano (I)

Phone: +39 02 503 24645

Fax: +39 02 503 24657

Email: francesco.cilurzo@unimi.it

Abstract:

This work aimed to design low-melting pressure sensitive adhesives and demonstrate the feasibility of the preparation of (trans)dermal patches by hot-melt ram extrusion printing. This approach allows defining both the geometry of (trans)dermal patch and the drug strength easily according to patient needs. The preparation steps are the mixing of a poly-ammonium methacrylate polymer (i.e. Eudragit RL and RS) with a suitable amount of plasticizer (triacetin or tributyl citrate) and the drug (ketoprofen or nicotine); the melting in the ram extruder and the printing on the backing layer foil. The formulations were characterized in terms of rheological and adhesive properties, *in vitro* drug release and skin permeation profiles.

The (trans)dermal patches made of Eudragit RL or Eudragit RS plasticized with the 40% triacetin could be printed at 90°C giving formulations with suitable adhesive properties and which did not exhibit cold flow after 1 month of storage at 40°C. Furthermore, the overall results showed that the performances of printed (trans)dermal patches overlapped those made by solvent casting, suggesting that the proposed solvent-free technology can be useful to treat cutaneous pathologies when the availability of (trans)dermal patches with a size and a shape that perfectly fit with the skin area affected by the disease improves the safety of the pharmacological treatment.

Keywords

Transdermal patches, Pressure-sensitive adhesive, Eudragit RL, Eudragit RS, Hot-melt extrusion, Printing.

1 Introduction

(Trans)dermal patches are well-known pharmaceutical preparations designed to be applied onto the skin surface for different purposes that range from the treatment of cutaneous pathologies to obtain a systemic effect (Cilurzo et al., 2014a). Independently of the final goal, the basic design of a (trans)dermal patch includes a backing layer, which protects the formulation from the outer environment, an adhesive matrix, which contains the drug and controls its release, and a protective foil, which is peeled out before the application of (trans)dermal patch (Wokovich et al., 2010). Usually, the adhesive matrices are made of soft thermoplastic polymeric materials able to adhere on the skin surface by simple contact under light pressure and to be peeled out without any residue. They are defined as pressure-sensitive adhesives (PSA) and can be directly synthesized for this purpose or compounded starting from pharmaceutical grade excipients (Cilurzo et al., 2008).

In particular, PSA used for the development of drug-loaded (trans)dermal patches by casting techniques are available on the market or compounded as water or organic solvent dispersions (Cilurzo et al., 2014b). Alternatively, hot-melt technologies could be applied since they allow a cheaper production of (trans)dermal patches (Wilson et al., 2012). Usually, the basic approach to produce a hot-melt PSA consists in the preparation of a blend in the hot mixer, in the transfer of the obtained PSA in suitable containers and its cooling. Afterwards, the required PSA amount is deposited in a heating container and, when melted, pumped onto the coater unit, which laminates the PSA on the release liner at the desired thickness. This approach is widely used in the production of medical devices, but it has been scantly investigated in the pharmaceutical field even if hot melt PSA could open new opportunities from both a formulation and preparation point of view. Then, the PSA laminated is associated with backing layer and cut to obtain the final shape and size of the (trans)dermal patch. Both hot-melt extrusion and solvent casting are semi-continuous manufacturing processes and, therefore, unsuitable either for scaling down the batch size or the personalization of the dose.

Consequently, when the market shares of a (trans)dermal patch are too low to ensure the economic sustainability of the manufacturing process, the access to therapies is jeopardized. In this case, the availability of a system suitable for the preparation of very small batches could be useful for the specific patient need. As an example, the production of scopolamine transdermal patches, which had been indicated for the treatment of motion sickness, was interrupted in the last years. This decision of the manufacturer has a substantial impact on patients affected by amyotrophic lateral sclerosis, who used the scopolamine transdermal patches as off-label treatment for managing the sialorrhea (Garuti et al., 2019).

The conventional 3D printing technologies cannot be applied to the preparation of (trans)dermal patches, since the pressure-sensitive adhesives are very soft and sticky and cannot be used for the production of pre-made filaments such those used for fused-deposition modelling (FMD) 3D printing. Only a few pieces of evidence on self-adhesive nanofiber networks have been reported (Shi et al., 2014).

This work explores the possibility to print of very small batch of (trans)dermal patches compatible with the extemporaneous preparation for specific patients. To demonstrate the feasibility of such a process we investigated the critical aspects related to the application of printing a melted PSA with a specific geometry on the backing layer of (trans)dermal patch. PSA made of Eudragit RL or RS, suitably plasticized by triacetin (TRI) or tributyl citrate (TBC), were used. These materials were selected since it was already demonstrated that the rheological properties of highly plasticized Eudragit RL are suitable for the preparation of PSA (Quaroni et al., 2018). Indeed, during the bonding phase (tack), these materials behave like a viscous liquid to favour its spreading onto the skin and to form good molecular contact under a lightly applied pressure. Conversely, during the debonding process from the skin (peel), the adhesive should behave like a cohesive solid to ensure complete removal without leaving any residue (O'Connor and Willenbacher, 2004). Furthermore, a (trans)dermal patch should remain attached to the skin for the entire treatment period, without any overspreading of the adhesive matrix beyond the boundaries. Therefore, it should also be highly

dissipative and lightly physically or chemically crosslinked to resist the applied stress once the bond is formed.

Keeping in mind these features, the formulation space was investigated by using different copolymers' ratio blended with different amounts of the selected plasticizers and their impact on the adhesive properties of (trans)dermal patch was also checked. Then, the suitability of the selected PSA for the preparation of (trans)dermal patches was tested by loading ketoprofen (KP) and nicotine (NT) and comparing their performances with those of analogous (trans)dermal patches prepared by casting (Quaroni et al., 2018).

The printing was performed according to a protocol already described for the preparation of orodispersible films (Musazzi et al., 2018b). Briefly, the preparation procedure is simple and consists in wetting the powders (i.e. the drug and the copolymer) with the plasticizer, loading the mixture in the printer and printing the melt directly on the backing layer. Afterwards, the (trans)dermal patches were coupled with the release liner and sealed in an airtight bag.

2 Materials and methods

2.1 Materials

Poly-(ethylacrylate-co-methylmethacrylate-co-trimethylammonioethylmethacrylate chloride), trade with the name Eudragit® RL PO (EuRL) and Eudragit® RS PO (EuRS), with a molar ratio of 1:2:0.2 and 1:2:0.1 respectively, were kindly donated by Rofarma Italia (I). Tributyl citrate (TBC) was supplied by Morflex (US), whereas triacetin (TRI) and NT were purchased from Sigma Aldrich (Milan, I). KP was purchased form Farmalabor (I). The release liner and the backing layers tested were kindly donated by Bouty S.p.A. (I). All solvents were of analytical grade unless specified.

2.2 Preparation of (trans)dermal patch

The mixtures were obtained by mixing the accurately weighted amount of each component in a mortar according to the composition reported in **Table 1** and **Table 2**. The final weight of each mixture was about 10 g.

The mixture was immediately transferred in the ram extrusion apparatus previously described (Musazzi et al., 2018b), melted and printed at 90°C through a 0.7-mm needle. The printer was designed modifying a Cartesian FDM 3D printer (Futura Group Srl, Italy), substituting the FDM apparatus with a home-made ram extrusion system. The distance from the needle tip to the surface of the backing layer was fixed at 0.3 mm to permit a suitable deposition of the melted blend, in a unique layer, and to obtain an adhesive matrix with a thickness around 50-70 μm. The speeds of the mobile plate and the extruder ram were set at 12 mm/s and 10 mm/s, respectively. Finally, the filling angle was set at 135° to the X-axis of the baking layer.

The melted materials extruded through the die was deposited on the 20 × 20 cm backing layer foil fixed in the Cartesian plate of the printer. The dimension and number of (trans)dermal patches per each print were set up by 3D builder® (Microsoft, US) and converted in G-code. Afterwards, the (trans)dermal patches were matched with a siliconized polyethene film sealed in the primary packaging and stored until use without further manipulations.

2.3 Rheological tests

The polymeric blends were prepared according to the procedure reported above. The sample was printed on a release liner having both the surface coated with a different layer of silicon and then covered with the same material. Afterwards, the sandwich was pressed to smooth the surface. The rheological properties of the formulations were assessed and reported in **Table 1**. The assays were conducted at 21 ± 0.2°C using a Physica MCR 302 rheometer (Anton Paar GmbH, A) with a cone-plate geometry of 1° incline, 50 mm diameter. Minimum plate gap was set at 100 μm. Before the

analyses, a strain test was performed to determine the linear viscoelastic range of the samples: after the test, shear strain for the experiments was set at 5%.

Frequency sweep experiments were performed, going from 0.01 rad/s to 100 rad/s, collecting 16 points in the range chosen, with logarithmic progression. The data were analysed as previously described (Quaroni et. al, 2018). The complex viscosity (η^*) determined at 1.5 Hz, and the crossover of G'/G" were determined as descriptors of the rheological pattern of the prepared PSA. In particular, the η^*, calculated according to the Eq. 1, was used to predict the steady shear viscosity according to the Cox-Merz rule, which states that the complex viscosity as a function of frequency is equivalent to the steady shear viscosity as a function of shear rate (Hicks et al. 2015):

$$\eta^* = \frac{G^*}{\omega} \quad (1)$$

where G* is the complex modulus at the established angular frequency (ω).

2.4 Thickness of (trans)dermal patch

The film thickness was measured by using a micrometer MI 1000 µm (ChemInstruments, US). The results were expressed as the mean ± standard deviation of five specimens for each formulation.

2.5 Optical microscopy

The overall morphology, the appearance of the printed patches (including crystal formation) were evaluated by optical microscopy with a stereomicroscope (Nikon, I). Micrographs were acquired at 10× magnification with a digital camera of 3.1 Mpx (CCD 3, ToupView, ToupTek, China).

2.6 Adhesive properties determination

The adhesive and cohesive properties of the printed (trans)dermal patches were tested applying standard procedures generally used for the characterization of (trans)dermal patches: cold flow, probe tack test, shear adhesion test and peel adhesion 180° test (Cilurzo et al., 2012; Quaroni et al., 2018).

Cold flow – The cold flow is one of the possible quality defects of (trans)dermal patches and represents the migration of a PSA outside the edge of the backing layer during the storage. This phenomenon can be observed when the matrix of (trans)dermal patch has a significant viscous-like behaviour to flow between the backing layer and release liner. The cold flow was evaluated on samples of 25 x 50 mm after a storage period of 1 month at room temperature (RT) or 40 ± 1°C. The sample complied with the test when the PSA was not visually detectable outside the backing layer. When occurring, the extent of cold flow was expressed as the maximum migration of the adhesive in millimetre on the release liner. It was measured putting the sample, which was in any case almost transparent, on a graph paper.

The analysis was performed in triplicate. If the cold flow was observed, the formulation was discarded.

Probe tack test – The tack adhesion test reveals the force of debonding the PSA matrix from a surface after a short contact time and applying light pressure. It is relevant for (trans)dermal patch since it allows to estimate the initial bonding of a PSA onto the application site. Briefly, (trans)dermal patches of 25 x 60 mm were printed from each formulation and stored at 25 ± 1°C for two weeks to assure the stabilization of the adhesive matrix (Quaroni et al., 2018). The probe tack test was performed according to a standard internal procedure using a tensile testing machine equipped with a 50 N cell (Instron 5965, ITW Test and Measurement Italia S.r.l., I). A strip of double-coated tape (TESA, D) having the same size of the plaster specimen was applied between the flat bottom plate of the tensile testing machine and the backing layer of the specimen. The release liner of (trans)dermal patch was then removed. The flat stainless-steel probe (diameter: 5 mm) was placed ~0.05 mm above the adhesive matrix. The probe was then lowered onto the adhesive surface, and a constant force of 0.05 N was applied onto the sample for 5 s and, finally, the probe was removed at the debonding rate of 0.1 mm/s. The absence of PSA residues on the probe surface (adhesive failure) was visually determined. The whole force-distance curve (compression and traction) was recorded. The area under

the curve force vs probe displacement was assumed as the work of separation (W). The tack stress (σ_{max}) values for each experiment were calculated as the maximum traction force normalized by the probe area. The results were expressed as the mean ± standard deviation of four determinations.

Shear adhesion test – The shear adhesion test reveals the resistance of a PSA matrix to tangential stress and, therefore, the cohesion of the matrix of (trans)dermal patch. Briefly, specimens of 25 x 60 mm were printed from each formulation (**Table 1** and **2**) and stored at 25 ± 1°C for two weeks to assure the stabilization of the adhesive matrix (Quaroni et al., 2018). The shear adhesion was performed using an 8 Bank Oven Shear HT8 Instrument (ChemInstruments, Ichemico, I) according to a method previously described using a 500 g mass to generate the stress. The experiments were performed at room temperature (25 ± 1 °C). The results were expressed as the mean ± standard deviation of four specimens.

Peel adhesion 180° test – The peel adhesion reveals the resistance of (trans)dermal patch to peeling-off. It has a crucial role in the characterization of (trans)dermal patch since high peel adhesion resulted in a more painful its removal from the skin by the patient. The tests were performed using a tensile machine equipped with a 50 N cell (Instron 5965, ITW Test and Measurement Italia S.r.l., I) using a Teflon® panel, accordingly to the method described by Cilurzo and co-workers (Cilurzo et al., 2008). (Trans)dermal patches printed with a 12 x 80 mm size were stored in primary packaging material at 25 ± 1°C for two weeks before use.

2.7 Drug content

An accurately weighed 2.54 cm^2 (trans)dermal patch was dissolved in 50 mL methanol by mechanically shaking and sonication (UP200st, Hielscher, D). Afterwards, the samples were left to rest overnight and, then, diluted 1:1 with mobile phase described below. Before the injection, samples were filtered with a 0.45 μm polypropylene filter (VWR International, I). The drug content in the

211 (trans)dermal patch was calculated as a function of both the matrix mass (μg/g) and area (μg/cm^2).
212 The results were expressed as the mean ± standard deviation of three specimens for each formulation.
213
214 **2.8 In vitro dissolution test**
215 The dissolution was performed by using an apparatus SR8 PLUS dissolution test station (Hanson
216 Research, US) according to the disk assembly method described in the "Dissolution test for
217 transdermal patches (01/2008:20904)" of European Pharmacopoeia.
218 An 8.0 cm^2 (trans)dermal patch was placed flat on the iron disk (mesh size of the disk net: 125 μm)
219 with the adhesive surface facing up according to the method previously described. The vessels were
220 filled with 300 mL of pH 7.4 PBS buffer, the water bath temperature was kept at 32.0 ± 0.5 °C, and
221 the paddle speed was set at 25 rpm. At predetermined intervals (5, 10, 20, 30 min, 1, 2, 4, 6, 7, 24 h),
222 5 mL samples were collected and immediately replenished with fresh medium.
223 The solutions were assayed by HPLC, according to the methods reported below. The results were
224 expressed as the mean ± standard deviation of three specimens for each formulation. The release rate
225 constant was calculated according to Higuchi's equation as follows:
226 $$M_t/M_\infty = Kt^{0.5} \quad (2)$$
227 where M_t is the amount of drug released at time t, M_∞ is the drug loading in the matrix and *K* is the
228 release rate constant expressed as h^{-1}.
229
230 **2.9 In vitro permeation studies**
231 The permeation studies were performed using abdominal skin from donors, who underwent cosmetic
232 surgery. According to an internal protocol (Casiraghi et al., 2016), after removing the subcutaneous
233 fatty tissue, the skin samples were immersed in water at 60 °C for 1 min, and the epidermis was
234 carefully removed from the underlying tissue with the help of forceps. The integrity of epidermis
235 samples was assessed measuring their electrical resistance (voltage: 100 mV, frequency: 100 Hz;
236 Agilent 4263B LCR Meter, Microlease, I), using a modified Franz diffusion cell (PermeGear, US)

with an effective permeation area and a receptor volume of 0.636 cm^2 and 3 mL, respectively. Samples with an electrical resistance higher than 20 $k\Omega \cdot cm^2$ were used for the in vitro permeation experiments (Cilurzo et al., 2018).

At the beginning of the *in vitro* permeation studies, a 2.5 cm^2 circular sample, obtained from a printed (trans)dermal patch by a precision die cutter, was gently applied to the epidermis specimen. Then, the assembly was mounted on the receiver compartment of the Franz diffusion cell filled with saline solution, containing sodium azide (100 μg/mL), as a preservative, and maintained at 35 ± 1 °C, so that the skin surface temperature was 32 ± 1 °C. Special care was taken to avoid air bubbles between the epidermis and the medium in the receptor compartment. The receptor medium was continuously stirred with a small magnetic bar at 1800 rpm to assure a uniform distribution of the permeated drug. The upper and lower parts of the Franz diffusion cell were sealed with Teflon (VWR International, I) and Parafilm® (Pechiney Plastic Packaging Company, US) and fastened together using a clamp. At predetermined times (1, 3, 5, 7, 24 h), 200 μL samples were withdrawn from the receiver compartment and replaced with fresh receiver medium. Sink conditions were maintained throughout the experiments. Samples were analysed by HPLC according to the methods described below. The cumulative amount (Q) permeated through the skin per unit of area was calculated from the concentration of each substance in the receiving medium and plotted as a function of time. The steady flux (J) was calculated as the slope of the linear portion of the plot.

2.10 HPLC method

The drug content and the drug concentration in the dissolution medium were quantified by HPLC analysis (Agilent HP 1100, Chemstation, Hewlett Packard, US), using the following analytical methods.

Ketoprofen – the following chromatographic conditions were used: column, HyperClone™ 5 μm BDS C18 130, 150x4.6 mm (Phenomenex, US); mobile phase, acetonitrile/water pH 2.6 (60/40, % v/v); flow rate, 1.5 mL/min; wavelengths, 225 nm; temperature, 25 °C; injection volume, 20μL. The

drug concentrations were determined from standard curves in the 0.1–50.0 μg/mL range (R^2 = 0.99999).

Nicotine – the following chromatographic conditions were used: column, Lichropher 110RP-18E, 125x4.0 mm, 5 μm (CPS Analitica, I) mobile phase, acetonitrile/KH_2PO_4 0.1M solution (25/75, % v/v) + 1.3 g/L sodium dodecyl sulphate; flow rate, 1.5 mL/min; wavelengths, 245 nm; temperature, 30 °C; injection volume, 20 μL. The drug concentrations were determined from standard curves in the 0.1–50.0 μg/mL range (R^2 = 0.99992).

3 Results and Discussion

3.1 Rheological pattern of designed formulations

Rheological analyses show common trends according to the formulation tested: as expected, increasing the plasticizer ratio, the viscosity gets lower with both TBC and TRI. **Fig. 1** shows the typical pattern of rheological analyses. As a general statement, EuRL formulations had higher viscosities in comparison to EuRS ones. This finding is probably due to a higher concentration of quaternary ammonium salt in EuRL, which increases ionic content and, consequently, the interactions with the polar groups of the plasticizer. A considerable difference between EuRL and EuRS is visible checking the crossover values, i.e. the frequency corresponding to the equivalence between loss (G'') and storage (G') modulus (**Table 1**). Accordingly, crossover occurs at higher frequencies when EuRS is used in comparison to the same formulations containing EuRL (**Table 1**), indicating that elastic modulus retains higher values for a higher range of frequencies. This different pattern confirmed the role of the percentages of ammonium groups present in the two copolymers. Interestingly, when using a 60/40 polymer/plasticizer ratio, a double crossover can be seen or expected, with the second crossover close to the highest frequency used for the analysis (100 rad/s).

The values of Tan δ (i.e. the G"/G' ratio) minimum agree with the trends of G" vs G', i.e. when EuRL and TBC are present, Tan δ minimum is visible at lower frequencies. When higher amounts of plasticizer are used, the minimum is out of the frequency range used for the analyses.

3.2 Selection of the pressure-sensitive adhesive composition

In agreement with the results of rheological analyses on polymeric blends, both the type of copolymer (i.e., EuRL or EuRS) and plasticizer (i.e., TBC or TRI) significantly impacted on the printability of the placebo (trans)dermal patches (**Table 1**). In particular, for EuRS, the use of both plasticizes in concentrations equal to 60% w/w resulted in too-fluid matrixes to be printable in a reproducible matter at the selected temperature. Moreover, the reduction of the extrusion temperature to 70°C resulted useless since the matrix flowed outside the edge of the (trans)dermal patch quickly after the application of the backing layer. EuRL showed a similar behaviour only when 60% w/w TRI was used. In the case of formulations designed with 40% w/w TBC the extrusion at 90°C led to a melt that was too stiff to adhere to the backing layer, so the temperature was increased up 100°C. These findings agreed with the complex viscosity (η*) of the polymeric blend at 25°C (1.5 Hz), even if such a temperature was significantly lower than extrusion one. The η*-values of EuRS-based (trans)dermal patches were lower than the equivalent EuRL formulations, justifying the worsening of the printability of (trans)dermal patch. Indeed, at equal plasticizer concentration, the EuRS matrices were more fluid than EuRL ones (**Table 1**). Moreover, TRI decreased more significantly the η*-value than TBC. These differences were more significant for EuRL-matrices (e.g., Form. **2** vs Form. **5**) than EuRS ones (e.g., Form. **8** vs Form. **10**). These results agreed with rheological results obtained on EuRL-based adhesive matrix prepared by solvent casting (Quaroni et al., 2018). Indeed, the rheological properties of EuRL/TRI-based matrices showed a more liquid-like behaviour than EuRL/TBC ones due to more significant interaction of TRI with polymeric chains.

The overall results suggested that η*-values lower than 1 KPa/s were correlated to a high fluidity of the extruded materials to be printed in a defined shape and size, whereas values higher than 15 KPa/s

to melt matrices too stiff to adhere to the backing layer and to obtain homogenous (trans)dermal patches (Form. **1**, **Table 1**). For η*-values ranged between 1 and 10 KPa/s, the formulations were printable in a reproducible matter.

Starting from these results, the impact of the copolymer ratio was also tested using 50% w/w TBC or 40% w/w TRI (Forms. **12-17**, **Table 1**). In these cases, all the formulations showed η*-values in the range of printability of (trans)dermal patch, even if a slight decrease was observed increasing the EuRS concentration within the matrix.

All the printed (trans)dermal patches resulted homogeneous (**Fig. 2**) with a reproducible thickness ranging 50 ± 10 μm. Nevertheless, several formulations showed a too high cold flow (**Table 1**). In particular, PSAs prepared with EuRL or EuRS with 60% w/w plasticizer failed the assay after one month of storage. This phenomenon occurs when, at low frequencies (in the range 0.05-0.5 rad/s), the G' values are relatively low, and G" ones are predominant. In the case of printed (trans)dermal patches, the cold flow was observed when η*-value was lower than 3 kPa/s (at 1.5 Hz), and the ratio between G' and tan δ determined at 0.4 rad/s was lower than 0.2 kPa (Rohn, 1959).

Moving the attention to the adhesive properties, accordingly to Class and Chu, optimal tack properties of the prepared placebo (trans)dermal patches may be reached with the G'-values between 5 x 10^4 and 2 x 10^5 Pa at frequencies between 0.005 and 0.05 rad/s (Rohn, 1959). In the case of printed (trans)dermal patches, the higher σ_{max} and W-values were observed with G'-values around 10^3-10^4 Pa, supporting the acceptable adhesive properties of the matrices. Moreover, the Dahlquist's criterion (G' ≤ 0.1 MPa at 1 Hz) was fulfilled by most of the formulations, suggesting that adhesive matrices were able to wet the adherend surface completely (Dahlquist, 1959). Indeed, exception made for Form. **1** which showed a weak adhesion property, all the formulations showed G'-values lower than 10^5 Pa (**Fig. 1**). The G'-values of EuRS-based matrices (≤ 10^3 Pa) are significantly lower than those of EuRL ones; however, the higher Tan δ values revealed a higher viscous behaviour of the former matrices (G''> G') at low frequencies. In the case of EuRL matrices, when 40% w/w TRI was used

as a plasticizer, the tack parameters resulted significantly higher than those obtained from TBC-containing matrices. However, this difference was significantly reduced, increasing the plasticizer concentration up to 50% w/w, due to a prevalence of the viscous behaviour of the materials (G''> G').

EuRL matrices showed higher shear adhesion than EuRS matrices (e.g., Form. **1** vs Form. **7**). This feature is in agreement with the rheological data showing a higher storage modulus (G') in EuRL matrices than in EuRS, at frequencies between 0.05 and 0.5 rad/s that is the range usually considered to predict the shear adhesion (**Fig. 1**) (Rohn, 1959).

The results of 180° peel adhesion tests demonstrated that the forces required to peel away all the printed (trans)dermal patches from the Teflon® surface were quite low. The type of plasticizer and copolymer composition did not influence peel value. This result could be due to the low critical surface tension of Teflon (Minghetti et al., 1999) which mimics the critical surface tension of the clean human skin and requires a low force for the detachment. On the other hand, the use of a substrate with a higher critical surface tension (i.e. steel) was tested but resulted not feasible since it caused an adhesive failure for several formulations (data not shown).

However, it is noteworthy that the overall results of peel tests suggested that printed (trans)dermal patches were more easy-to-peel than styrene-based matrices prepared with other hot-melt extrusion techniques (Ma et al., 2013; Zhao et al., 2016).

In the case of EuRL/EuRS blends, the tack (σ_{max} and W-values, **Table 1**) was influenced by the EuRS concentration. In agreements with results obtained for EuRL and EuRS blends, the effects varied as a function of the plasticizer type. In the presence of TBC, the higher the EuRS concentration, the higher the σ_{max} and W-values (Forms. **12-14**, **Table 1**). On the contrary, the opposite trend was observed for TRI-based formulations (Forms. **15-17**, **Table 1**).

The shear adhesion studies showed a low cohesivity of the TBC-contained matrices, whereas acceptable values were observed in the presence of TRI. Indeed, the shear adhesion of TRI-based (trans)dermal patches (>140 min) was 7-fold higher than TBC-based ones (< 20 min). Although the data of TRI series were lower than those obtained with other polymeric matrices prepared with hot-melt extrusion techniques (Ma et al., 2013; Zhao et al., 2016), they agreed with those available in the literature for marketed loco-regional patches (Cilurzo et al., 2015), whereas are significantly higher than those obtained by nanofiber patches prepared by electrospinning (Shi et al., 2014). Moreover, a direct correlation between the matrix resistance to flow and the EuRL/EuRS ratio was found. Indeed, comparing matrices containing the same plasticizer, the higher the EuRL concentration, the higher the shear adhesion value (R^2 = 0.87). This finding agreed with data published by Quaroni and co-workers (Quaroni et al., 2018). The overall data confirms that the proposed preparation method does not affect the adhesive performances of the (trans)dermal patches in comparison to the consolidated solvent casting technique.

3.3 Drug-loaded (trans)dermal patches

Considering the pattern exhibited by placebo (trans)dermal patches, both KP and NT were loaded on adhesive matrixes starting from the placebo formulations prepared using the 40% w/w TRI (**Table 2**).

The loading of KP and NT did not affect the printing of the (trans)dermal patches, and they were reproducible enough to fulfil with the Ph Eur monograph on the uniformity of content (**Table 3**). Moreover, the PSA appears homogeneous without a sign of crystallization grown (**Fig. 2**). Neither for KP nor NT, no morphological differences were observed between the drug-loaded and placebo PSA. After the process, no significant degradation pattern of both KT and NT have been detected. Although a deepened characterization of the physical state of both drugs was not performed, the experimental data suggested no significantly variations were expectable based on previous evidence

reported on the literature obtained with PSA-matrixes made of the same PSA (Cilurzo et al., 2008; Quaroni et al., 2018).

When both drugs were loaded in the adhesive matrices, the fluidity of the extruded material was increased, facilitating the printing of (trans)dermal patch. This evidence is also related to a reduction of the shear adhesion values in comparison to placebo printed (trans)dermal patches (**Table 2**). For examples, the shear adhesion value of Form. **16** (234 ± 45 min) decreased up to 3-fold and 9-fold when KP (Form. **16-KP**: 64 ± 11 min) and NT (Form. **16-NT**: 25 ± 5 min) was loaded in the matrix, respectively ($p < 0.05$, Student's T-Test). However, the observed reduction should have no impact on the *in vitro* performances of the printed (trans)dermal patch onto patient skin since the observed values remained comparable to other marketed cutaneous patches and medicated plasters (Minghetti et al., 1999).

The *in vitro* release studies demonstrated that the release profiles from EuRL/EuRS matrices depended on the type of loaded drug. Indeed, as shown in **Fig. 3**, the NT was released faster than KP from the same adhesive matrices. For example, 80% of NT was released in less than 30 min from Form. **4-NT**, whereas KP in 4 hours from the same adhesive matrix (Form. **4-KP**). This evidence was in line with published papers that had demonstrated the chemical interactions between KP and acrylic copolymer and their impact on the physicochemical features and the technological performance of the drug-loaded dosage form (Eerikäinen et al., 2004; Musazzi et al., 2018a; Rassu et al., 2008).

Besides these results, it is noteworthy that the released rate constant of KP from Form. **4-KP** (**Table 3**) resulted slightly smaller but comparable to that obtained from a (trans)dermal patch with a similar composition but prepared by solvent casting technique [$K = 0.78 \pm 0.01$ h^{-1} (Quaroni et al., 2018)]. These similarities in release profile suggested that, also for this property, the changes in preparation methods did not alter the ability of the matrix in released the loaded drug. Moreover, the *in vitro* drug release profiles also confirmed the role of copolymer ratio on the release of the drug through the matrices. It is noteworthy that EuRL matrix was more permeable to water and drugs than EuRS (Akhagari et al., 2006; Cilurzo et al., 2014a). The observed differences are also ascribable to a higher

swelling in aqueous solvents of EuRL compared to EuRS, especially around neutral pH (Akhagari et al., 2006). As shown in **Table 3**, the higher the EuRL concentration in the matrix, the higher the release rate constants. Indeed, regardless the loaded drug, the release rate constants increased in the following order: EuRL/EuRS 0/1 (Forms. **9-KP**, **9-NT**) < EuRL/EuRS 1/1 (Forms. **16-KP**, **16-NT**) < EuRL/EuRS 1/0 (Forms. **4-KP**, **4-NT**).

These results agreed with literature regarding the influence of EuRL/EuRS ratio on the *in vitro* and *in vivo* performances of (trans)dermal patches (Aggarwal et al., 2013; Cilurzo et al., 2014a; Kusum Devi et al., 2003; Mutalik and Udupa, 2004). Indeed, according to the well-known characteristics of the two copolymers, the higher the concentration of EuRL in the matrix, the higher the permeability of the matrix and, therefore, the higher the release rate of drugs. This effect is independent of the physicochemical properties of the drug substance loaded in the matrix. Indeed, the addition of EuRS to the formulation of (trans)dermal patch altered the diffusion/release mechanism of the drug. In particular, 20% of EuRS can reduce the diffusion of verapamil significantly through a EuRL-based adhesive matrix (Kusum Devi et al., 2003). Mutalik and Udupa confirmed this trend (Mutalik and Udupa, 2004). From EuRL/EuRS-based transdermal patches, the drug release of glibenclamide, a well-known hypoglycemic drug, was reduced when the EuRS concentration increased from 25% to 60% w/w.

It is noteworthy that the differences observed in the *in vitro* release profiles are not relevant in terms of skin permeation of KP (**Fig. 4**). Indeed, even if the release rate constant of EuRL-based (trans)dermal patches (Form. **4-KP**) resulted in more than two-time higher than EuRS-based (trans)dermal patches (Form. **9-KP**), the permeation fluxes were superimposable (**Table 3**). Such results are comparable to those obtained by other medicated plasters, regardless of the matrix composition (Cilurzo et al., 2015; Quaroni et al., 2018) and agree with the general statement that the permeation process is mainly related to the drug thermodynamic activity in the formulation (EMA, 2014). Indeed, the limiting step of drug permeation is the drug partition in the *stratum corneum* and not the drug release from the matrix. Therefore, the observed differences in the release rate of both

drugs may have a negligible impact on the actual concentration gradient between the outer and inner layers of the human epidermis, which is the real driving force of the permeation process. These considerations also justify the permeation pattern of NT (**Fig. 4**). In this case, the EuRS-based matrix permitted a high permeation (Form. **9-NT**; Q_{24} = 387.12 ± 29.10) in comparison to EuRL-based matrix (Form. **4-NT**; Q_{24} = 215.48 ± 38.56) in contrast with the dissolution data (**Table 3**). In agreement with the data discussed above, the decrease of the permeation flux of NT released by EuRL-based matrix observed after seven hours was attributed to a variation of the drug thermodynamic activity over time. The obtained results agreed with previously published data obtained from a similar polymeric matrix (Cilurzo et al., 2008).

4 Conclusions

The printing of hot-melt PSA based on poly-ammonium methacrylates, such as EuRL, EuRS and mixtures thereof, can be advantageously used for preparing or prototyping transdermal patches or medicated plasters. The selection of polymer/plasticizer ratio and the composition of other excipients can be easily optimized and controlled to guarantee suitable adhesive properties of the matrix and its stability during the time. Interestingly, the biopharmaceutical performances of the (trans)dermal patch (i.e., skin permeation) were not altered within the investigated formulative space, suggesting the high robustness of the proposed technology. Also, the obtained results evidenced that the performances of the printed (trans)dermal patches loaded with KP or NT are very close to that obtained by the conventional casting technique. Thus, the hot-melt ram extrusion printing can be a feasible technology in the production of very small batches for preliminary formulative studies, or preclinical/exploratory trials during the pharmaceutical development of a medicinal product. Moreover, it could be useful in the compounding of personalized cutaneous patches when the treatment of skin diseases requires original patch shape.

In conclusion, printing technologies can be advantageously used to produce small batches of (trans)dermal patches even if they require PSA appositely designed. As in the example reported in the actual study, the use of a hot-melt printing technique requires a material which exhibits a suitable viscosity to be printed at relatively lower temperatures than those generally required by a hot-melt extrusion process (Thakkara et al. 2020), and acquires suitable viscoelastic performances at room temperature to avoid cold flow and show acceptable adhesive properties. Starting from this proof-of-concept, further studies are required to better investigate the impact of the printing on the chemical and physical state of drug substances loaded in the (trans)dermal patches.

Figures

Fig. 1 Evolution of G' (solid line), G'' (long-dashed line) and Tan δ (dotted line) as a function of frequency. (A) EuRL patch formulations containing TRI and (C) TBC; (B) EuRS patch formulations containing TRI and (D) TBC. Black line: formulations containing 40% w/w of plasticizer, grey line: formulations containing 50% w/w of plasticizer and light grey line: formulations containing 40% w/w of plasticizer. Tests were performed at 25°C.

Fig. 2 Printed (trans)dermal patch during peeling off from the release liner (PSA: pressure-sensitive adhesive matrix; BL: backing layer; RL: release liner) (A) and microscopic image of KP-loaded patches (Form 4-KP), adhesive matrix plus backing layer, after removal of release liner (B). The image was taken on printed patched stored at room temperature for six months. No signs of crystallization were observable. The black spots detectable in the background belong to the intrinsic opacity of backing layer.

Fig. 3 In vitro release profiles of KP- (A) and NT-loaded patches (B) (Mean ± St.Dev.; n =3). Solid squares and lines: Forms **4-KP** and **4-NT**; Solid rhombus and dashed lines: Forms. **16-KP** and **16-NT**; Solid circles and dotted lines: Forms. **9-KP** and **9-NT**.

Fig. 4 In vitro permeation profiles of KP- (A) and NT-loaded patches (B) (Mean ± St.Dev.; n =3). Solid squares and lines: Forms **4-KP** and **4-NT**; Solid circles and dotted lines: Forms. **9-KP** and **9-NT**.

References

Aggarwal, G., Dhawan, S., Harikumar, S.L., 2013. Formulation, in vitro, and in vivo evaluation of matrix-type transdermal patches containing olanzapine, Pharm. Dev. Technol. 18, 916-925.

Akhgari, A., Farahmand, F., Afrasiabi Garekani, H., Sadeghi, F., Vandamme, T.F., 2006. Permeability and swelling studies on free films containing inulin in combination with different polymethacrylates aimed for colonic drug delivery, Eur. J. Pharm. 28, 307-314.

Casiraghi, A., Musazzi, U.M., Rocco, P., Franzè, S., Minghetti, P., 2016. Topical Treatment of Infantile Haemangiomas: A Comparative Study on the Selection of a Semi-Solid Vehicle, Skin Pharmacol. Physiol. 29, 210–219.

Cilurzo, F., Minghetti, P., Pagani, S., Casiraghi, A., Montanari, L., 2008. Design and characterization of an adhesive matrix based on a poly(ethyl acrylate, methyl methacrylate), AAPS PharmSciTech 9, 748-754.

Cilurzo, F., Selmin, F., Gennari, C.G.M., Montanari, L., Minghetti, P., 2014a. Application of methyl methacrylate copolymers to the development of transdermal or loco-regional drug delivery systems, Expert Opin. on Drug Deliv. 11, 1033-1045.

Cilurzo, F., Minghetti, P., Gennari, C.G.M., Casiraghi, A., Selmin, F., Montanari, L., 2014b. Formulation study of a patch containing propranolol by design of experiments, Drug Dev. Ind. Pharm. 40, 17-22.

Cilurzo, F., Gennari, C.G.M., Selmin, F., Franzé, S., Musazzi, U.M., Minghetti, P., 2015. On the characterization of medicated plasters containing NSAIDs according to novel indications of USP and EMA: adhesive property and in vitro skin permeation studies, Drug Dev. Ind. Pharm. 41, 183–189.

Cilurzo, F., Musazzi, U.M., Franzè, S., Fedele, G., Minghetti, P., 2018. Design of in vitro skin permeation studies according to the EMA guideline on quality of transdermal patches, Eur. J. Pharm. Sci. 125, 86-92.

Dahlquist, C.A., 1959. Creep. In: Satas D. (Ed.) Handbook of Pressure Sensitive Adhesive Technology, 3rd Edition. Satas and associates, Warwick, 121-138.

Eerikäinen, H., Peltonen, L., Raula, J., Hirvonen, J., Kauppinen, E.I., 2004. Nanoparticles containing ketoprofen and acrylic polymers prepared by and aerosol flow reactor method, AAPS PharmSciTech 5, 1-9.

EMA. Guideline on quality of transdermal patches (EMA/CHMP/QWP/608924/2014). London, 2014.

Garuti, G., Rao, F., Ribuffo, V., Sansone, V.A., 2019. Sialorrhea in patients with ALS: current treatment options, Degener. Neurol. Neuromuscul. Dis. 9, 19–26.

Hicks, C.R., Blair, E. Carlson, B.E., Mallick, P.K., 2015. Rheological study of automotive adhesives: Influence of storage time, temperature and shear rate on viscosity at dispensing, International J. Adh Adh, 63: 108-116.

Kusum Devi, V., Maria, G.R., Deepti, P.U., 2003. Design and Evaluation of Matrix Diffusion Controlled Transdermal Patches of Verapamil Hydrochloride, Drug Dev. Ind. Pharm. 29, 495-503.

Ma, J., Wnag, C., Luo, H., Zhu, Z., Wu, Y., Wang, H., 2013. Design and Evaluation of a Monolithic Drug-in-Adhesive Patch for Testosterone Based on Styrene–Isoprene–Styrene Block Copolymer, J. Pharm. Sci. 102, 2221-2234.

Minghetti, P., Cilurzo, F., Montanari, L., 1999. Evaluation of adhesive properties of patches based on acrylic matrices, Drug Dev. Ind. Pharm. 25, 1-6.

Musazzi, U.M., Selmin, F., Franzè, S., Gennari, C.G.M., Rocco, P., Minghetti, P., Cilurzo, F., 2018a. Poly(methyl methacrylate) salt as film forming material to design orodispersible films, Eur. J. Pharm. Sci. 115, 37-42.

Musazzi, U.M., Selmin, F., Ortenzi, M.A., Mohammed, G.K., Minghetti, P., Cilurzo, F., 2018b. Personalized orodispersible films by hot melt ram extrusion 3D printing, Int. J. Pharm. 551, 52-59.

Mutalik, S., Udupa, N., 2004. Glibenclamide Transdermal Patches: Physicochemical, Pharmacodynamic, and Pharmacokinetic Evaluations, J. Pharm Sci. 93, 1577-1594.

O'Connor, A.E., Willenbacher, N., 2004. The effect of molecular weight and temperature on tack properties of model polyisobutylenes, Int. J. Adhes. Adhes. 24, 335-346.

Quaroni, G.M.G., Gennari, C.G.M., Cilurzo, F., Ducouret, G., Creton, C., Minghetti, P., 2018. Tuning the rheological properties of an ammonium methacrylate copolymer for the design of adhesives suitable for transdermal patches, Eur. J. Pharm. Sci. 111, 238-246.

Rassu, G., Gavini, E., Spada, G., Giunchedi, P., Marceddu, S., 2008. Ketoprofen Spray-dried Microspheres Based on Eudragit® RS and RL: Study of the Manufacturing Parameters, Drug Dev. Ind. Pharm. 34, 1178-1187.

Rohn, C.L., 1959. Rheology of pressure sensitive adhesive. In: Satas D. (Ed.) Handbook of Pressure Sensitive Adhesive Technology, 3rd Edition. Satas and associates, Warwick, 153-170.

Shi, Y., Li, Y., Wu, J., Wang, W., Dong, A., Zhang, J., 2014. A novel transdermal drug delivery system based on self-adhesive Janus nanofibrous film with high breathability and monodirectional water-penetration. Journal of Biomaterials Science, Polymer Edition, 25(7), 713–728.

562 Thakkara, R., Thakkara, R., Pillaia, A., Ashoura, E.A., Repkaa, M.A., 2020. Systematic screening of
563 pharmaceutical polymers for hot melt extrusion processing: a comprehensive review. Int. J.
564 Pharm., 576, 118989.

565 Wilson, M., Williams, M.A., Jones, D.S., Andrews, G.P., 2012. Hot-melt extrusion technology and
566 pharmaceutical application, Ther. Deliv. 3, 787-97.

567 Wokovich, A.M., Shen, M., Doub, W.H., Machado, S.G., Buhse, L.F., 2010. Release liner removal
568 method for transdermal drug delivery systems (TDDS), J Pharm. Sci. 99, 3177-3187.

569 Zhao, Z., Zhou, Y., Zhang, C., Li Z., 2016. Optimization of SIS-based hot-melt pressure-sensitive
570 adhesives for transdermal delivery of hydrophilic drugs, Int. J. Adhes. Adhes. 68, 256-262.

571

Table 1 Composition (%) of placebo patches used for screening the acceptable polymer/plasticizer ratio in terms of matrix printability, cold flow after one month of storage, rheological and adhesive properties. The matrix printability is expressed by the following score system: A (easily printable), B (printable not in a reproducible way), and C (not printable). For cold flow: N, the absence of cold flow; Y, the presence of cold flow.

Form	Composition (%)				Printability	Rheological properties			Adhesive properties			
	EuRL	*EuRS*	*TBC*	*TRI*		*Cold flow*[1]	*η* (kPa/s)*[2]	*Cross over (rad/s)*	*Tack*		*Shear adhesion (min)*	*Peel adhesion (cN/cm)*
									σ_{max} *(kPa)*	*W (mJ)*		
1	60	-	40	-	B	N	20.5	0.1	5.9±1.5	0.008±0.001	2062±1124	12.8±5.1
2	50	-	50	-	A	N	6.1	0.4	246.8±61.2	0.105±0.023	157±43	15.2±2.1
3	40	-	60	-	A	Y	1.6	2.2	-[3]	-[3]	-[3]	-[3]
4	60	-	-	40	A	N	11.5	0.2	218.0±17.0	0.053±0.013	396±79	12.5±0.5
5	50	-	-	50	B	N	4.0	2.5	252.5±49.7	0.065±0.038	170±20	3.5±2.4
6	40	-	-	60	C	Y	1.0	13.5	-[3]	-[3]	-[3]	-[3]
7	-	60	40	-	A	N	10.9	1.0; 17.6	292.2±43.3	0.193±0.060	553±385	50.3±19.5
8	-	50	50	-	B	Y	2.4	>100	-[3]	-[3]	-[3]	-[3]
9	-	60	-	40	B	N	7.6	3.4	125.2±85.3	0.093±0.059	181±10	14.2±2.9
10	-	50	-	50	B	Y	2.0	40.0	-[3]	-[3]	-[3]	-[3]
11	-	40	-	60	C	Y	0.5	> 100	-[3]	-[3]	-[3]	-[3]
12	37.5	12.5	50	-	A	N	4.2	25.0	167.1±35.7	0.068±0.025	17 ± 4	12.8±7.9
13	25	25	50	-	A	N	5.6	> 100	114.2±24.7	0.067±0.017	5±1	7.4±0.9
14	12.5	37.5	50	-	B	N	2.9	> 100	7.5±5.4	0.022±0.012	8±1	7.4±0.5
15	45	15	-	40	A	N	10.1	0.9	8.5±0.9	0.006±0.001	364±149	7.4±1.1
16	30	30	-	40	A	N	7.3	2.5	87.6±32.2	0.046±0.016	234±45	10.3±1.0
17	15	45	-	40	B	N	4.6	44.0	214.5±49.3	0.093±0.016	149±41	15.3±0.7

[1] 40°C, 1 month; [2] determined at 1.5 Hz; [3] not determined since the cold flow was observed

Table 2 Composition (%) of drug-loaded patches, thickness, and their characterization in term of cold flow after one month at 25°C or at 40°C, and adhesive properties (N: the absence of cold flow; Y: the presence of cold flow).

Form.	**Composition (%)**						**Thickness (*μm*)**	**Cold flow**		**Adhesive properties**	
	EuRL	*EuRS*	*TBC*	*TRI*	*KP*	*NT*		*25°C*	*40°C*	*Shear adhesion (min)*	*Peel adhesion (cN/cm)*
4-KP	58.60	-	-	39.06	2.34	-	54 ± 8	N	Y	66 ± 3	7.7 ± 0.4
9-KP	-	58.60	-	39.06	2.34	-	58± 14	N	Y	67 ± 3	14.9 ± 5.8
16-KP	29.30	29.30	-	39.06	2.34	-	59 ± 11	N	Y	64 ± 11	13.5 ± 1.3
4-NT	58.20	-	-	39.06	-	3.00	62 ± 13	N	N	81 ± 3	5.3 ± 0.4
9-NT	-	58.20	-	39.06	-	3.00	67± 9	N	N	21 ± 8	12.0 ± 0.7
16-NT	29.10	29.10	-	39.06	-	3.00	66 ± 16	N	N	25 ± 5	9.4 ± 0.8

Table 3 Drug content, release rate constant (*K*) and skin permeation flux (*J*) of printed drug-loaded patches (Mean ± St.Dev.; n = 3; n.d.: not determined).

Form.	**Drug**	**Drug content**		***K***	***J***
		μg/mg	*μg/cm²*	**($h^{-0.5}$)**	**(μg/cm²/h)**
4-KP	KP	2.2 ± 0.1	166.1 ± 8.3	0.41 ± 0.02	0.60 ± 0.02
9-KP	KP	2.3 ± 0.0	152.1 ± 29.4	0.13 ± 0.01	0.60 ± 0.13
16-KP	KP	2.3 ± 0.1	161.7 ± 15.8	0.15 ± 0.01	n.d.
4-NT	NT	2.3 ± 0.1	158.6 ± 35.1	2.61 ± 0.05	15.28 ± 3.07
9-NT	NT	3.0 ± 0.5	196.6 ± 12.2	0.29 ± 0.07	20.38 ± 3.13
16-NT	NT	2.2 ± 0.4	136.5 ± 13.7	1.36 ± 0.09	n.d.

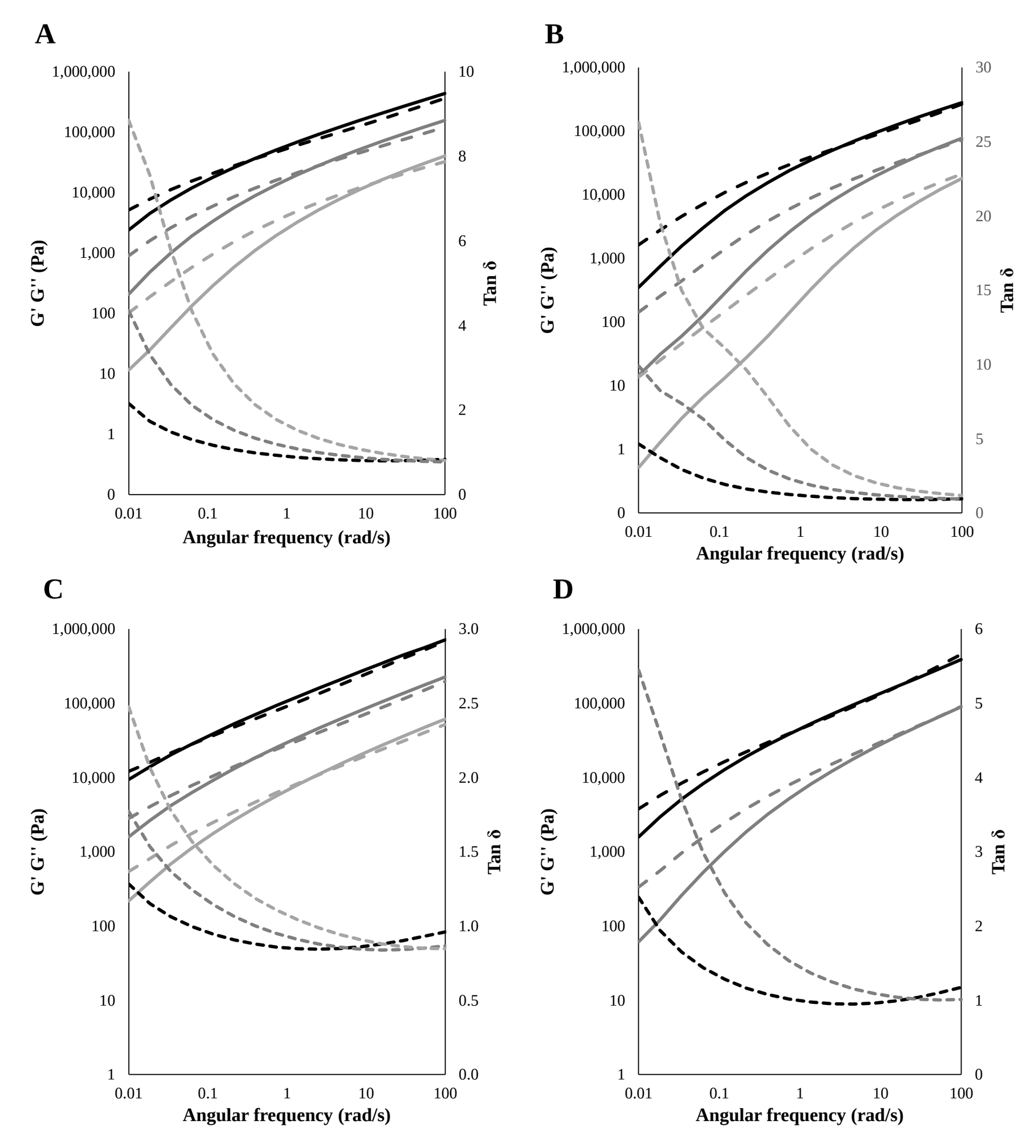
A
1,000,000
100,000
10,000
1,000
100
10
1
0
G' G'' (Pa)
10
8
6
4
2
0
Tan δ
0.01
0.1
1
10
100
Angular frequency (rad/s)
B
1,000,000
100,000
10,000
1,000
100
10
1
0
G' G'' (Pa)
30
25
20
15
10
5
0
Tan δ
0.01
0.1
1
10
100
Angular frequency (rad/s)
C
1,000,000
100,000
10,000
1,000
100
10
1
G' G'' (Pa)
3.0
2.5
2.0
1.5
1.0
0.5
0.0
Tan δ
0.01
0.1
1
10
100
Angular frequency (rad/s)
D
1,000,000
100,000
10,000
1,000
100
10
1
G' G'' (Pa)
6
5
4
3
2
1
0
Tan δ
0.01
0.1
1
10
100
Angular frequency (rad/s)

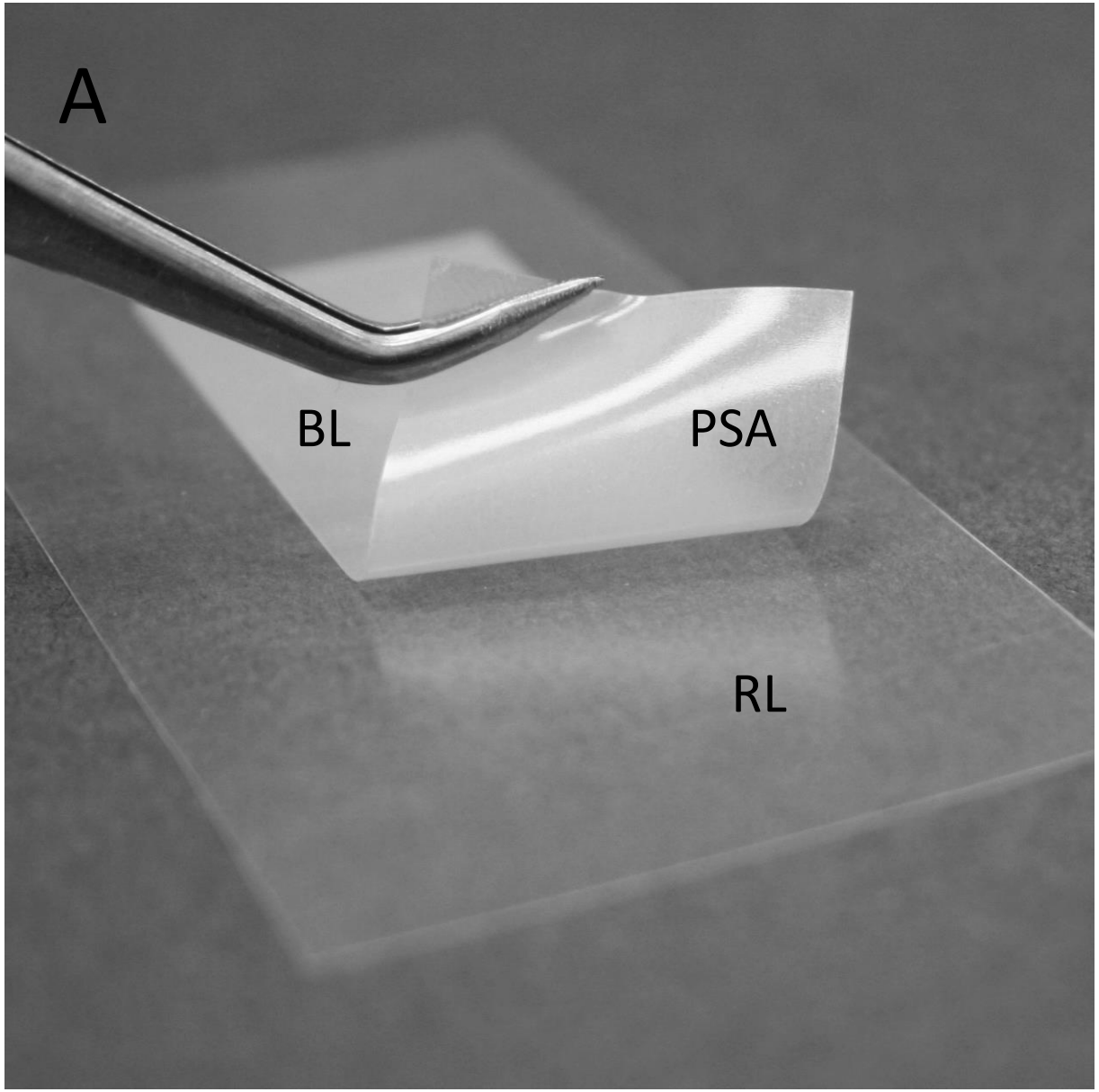
A
BL
PSA
RL

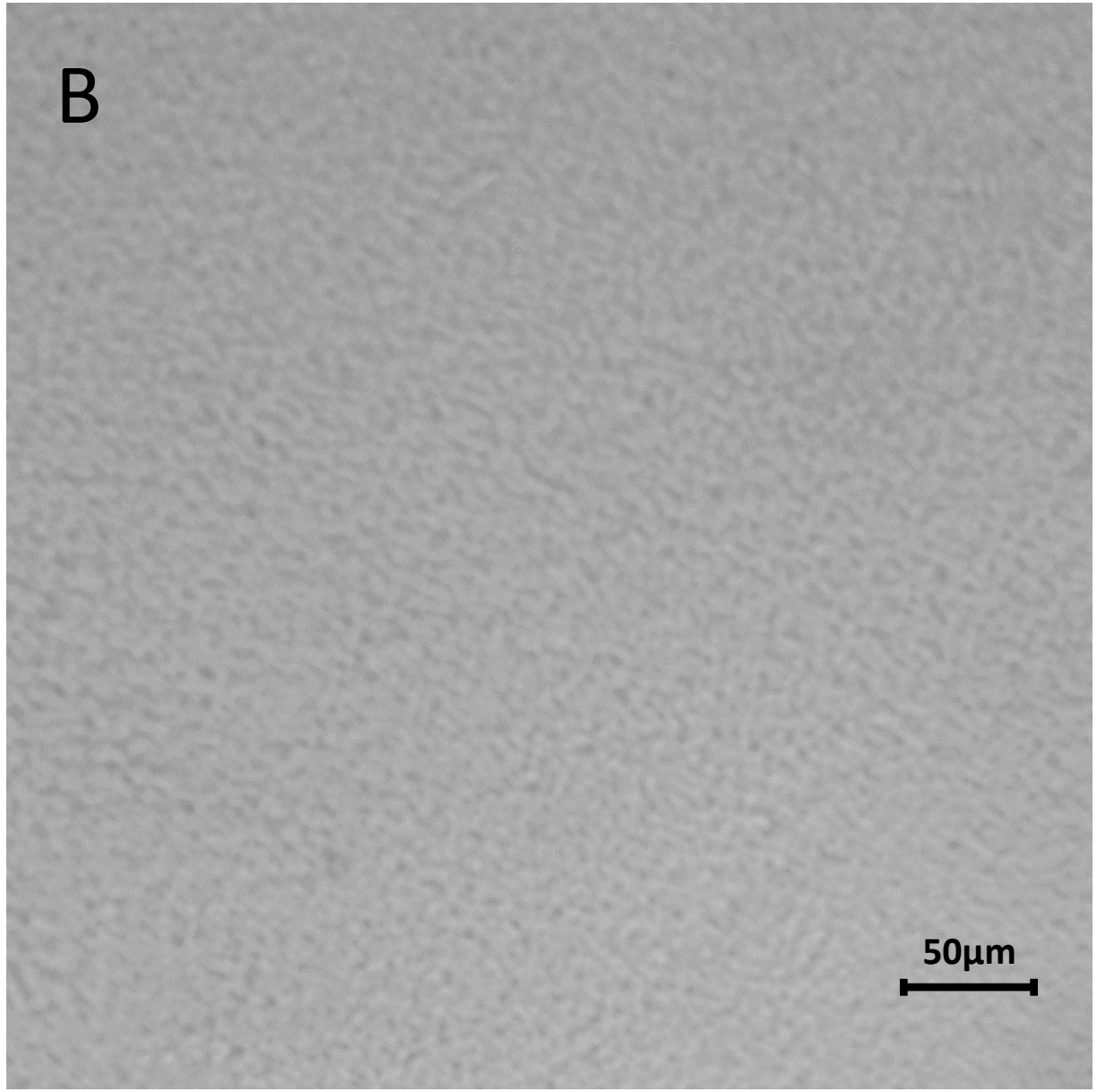
B
50µm

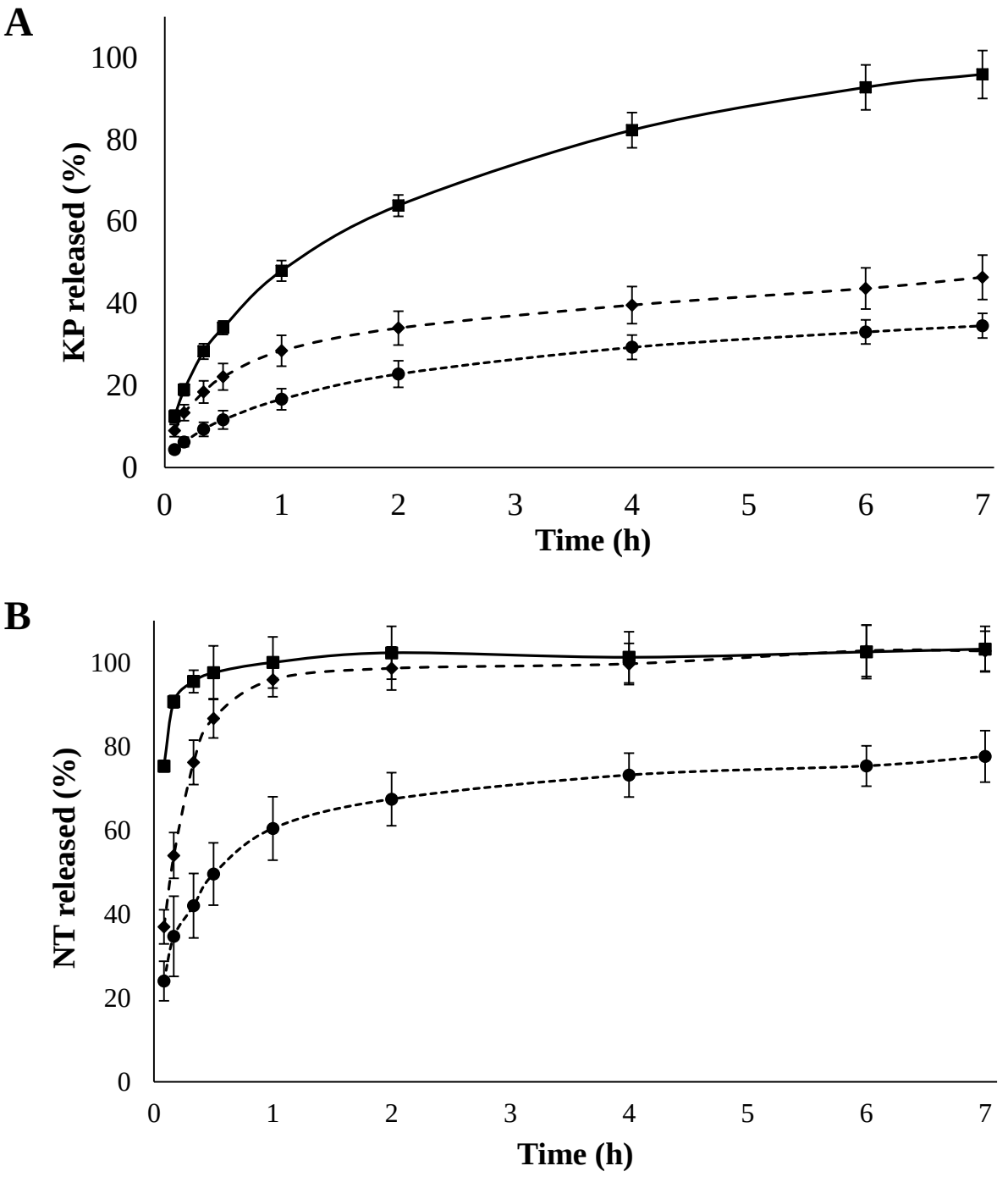
A
100
80
60
40
20
0
KP released (%)
0
1
2
3
4
5
6
7
Time (h)
B
100
80
60
40
20
0
NT released (%)
0
1
2
3
4
5
6
7
Time (h)

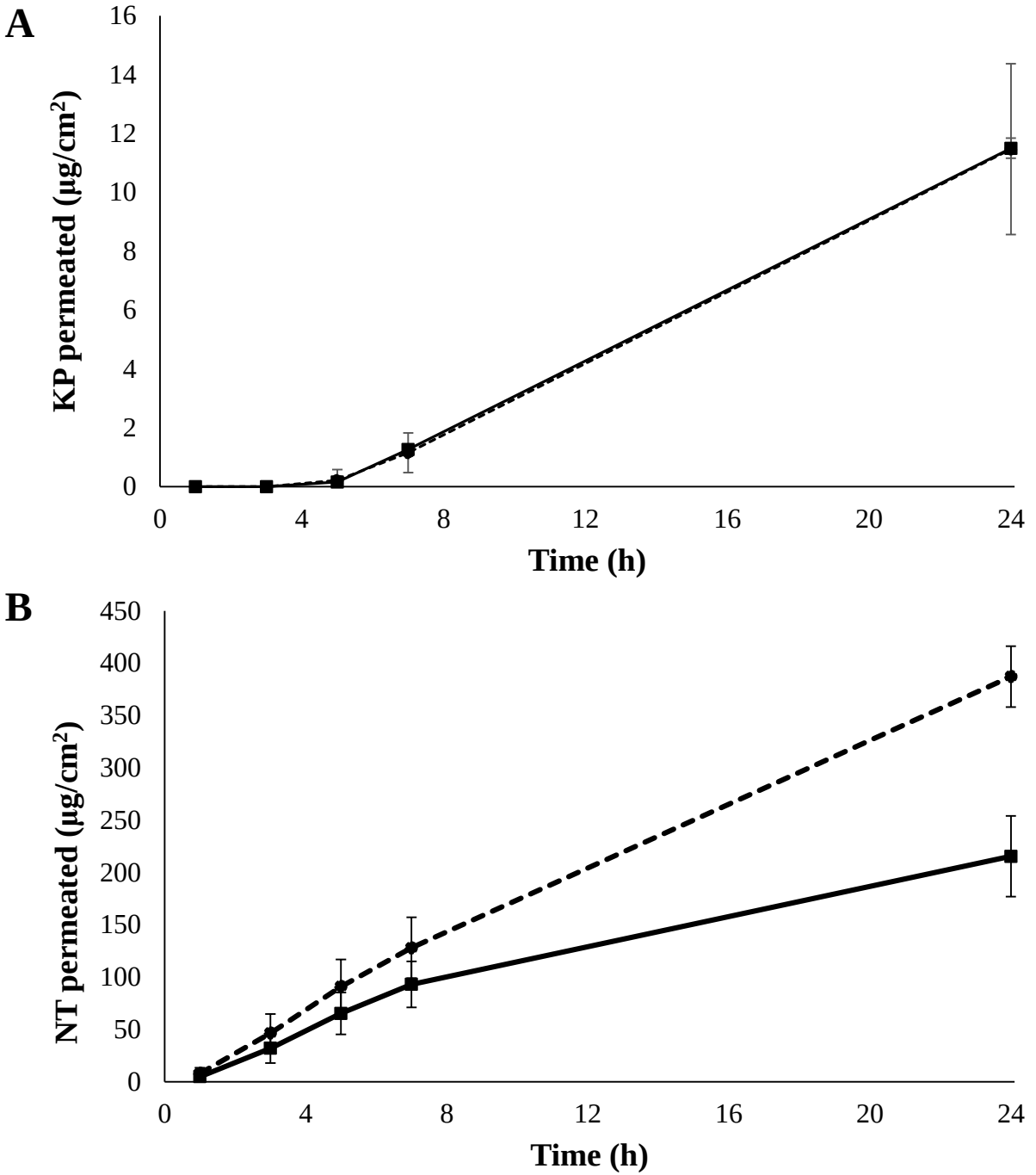
A
KP permeated (µg/cm²)
0
2
4
6
8
10
12
14
16
0
4
8
12
16
20
24
Time (h)
B
NT permeated (µg/cm²)
0
50
100
150
200
250
300
350
400
450
0
4
8
12
16
20
24
Time (h)